GLOBAL COOLING AND MASS EXTINCTION AT THE END OF THE CRETACEOUS PERIOD DRIVEN BY A DARK CLOUD ENCOUNTER. T. Nimura[1], T. Ebisuzaki[2], and S. Maruyama[3] , [1]Japan Spaceguard Association (1716-3 Okura, Bisei, Ibara, Okayama 714-1411, JAPAN, nimura@spaceguard.or.jp), [2]RIKEN (2-1, Hirosawa, Wako, Saitama 351-0198, JAPAN, ebisu@postman.riken.jp), [3]Earth-Life Science Institute, Tokyo Institute of Technology, 2-12-1-IE-1, Ookayama, Meguro-ku, Tokyo 152-8550, JAPAN, smaruyam@geo.titech.ac.jp).

Introduction: Maruyama and Santosh (2008) [1] suggested that some Earth's dramatic environmental changes are controlled by trigger in outer the Earth, solar system, or/and Galaxy. Kataoka et al (2013; 2014) [2, 3] pointed that the encounter with a dark cloud may drive environmental catastrophe to lead a mass extinction. A nebula encounter leads to a global cooling by the enhanced flux of cosmic dust particles.

We found the evidence of a dark nebula encounter in an ~5 m-thick section of pelagic sediment cored in the deep sea floor, in addition to a distinct spike in iridium at the K-Pg boundary related to the Chicxulub asteroid impact.

Samples: Through the Ocean Drilling Program (ODP), a core sample of pelagic sediment was taken at Site 886C, at a water depth of 5713.3 m in the central North Pacific (44°41.384´N, 168°14.400´W). Kyte et al. (1995) [4] measured the iridium and cobalt density in the core sample of Site 886C at a depth of 0.75-72.2 meters below the sea floor (mbsf) with a pelagic-sedimentation record extending from the Late Cretaceous (77.77 Ma at 71.60 mbsf) to the Late Miocene (9.8 Ma at 54.6 mbsf) (Fig 1b). The age of sediment was determined based on Sr-isotope stratigraphy below 54 mbsf of 886C [5].

Co-Ir diagram: The iridium abundance is plotted against cobalt abundance in Fig. 2, normalized by those of CI-chondrite. The large open squares represent Earth's surface materials (i.e., marine organisms [6, 7], earth crust [8], pelagic clays [9, 10], and manganese nodule [11-13]. The large solid squares represent CI chondrite [14]. The cobalt abundance of pelagic clays is used 222±41 ppm [10] as similar to 886C sample which are slow sedimentation rate (< 1m / Myr) and deep (> 5000 mbsf) sea sediment. The positive and negative error value for iridium and cobalt abundance for crust are adopted upper and lower crust [8]. Any mixtures of the Earth's surface materials must distribute in the gray area taken into account the measurement errors (3σ in iridium abundance: The standard deviation of the iridium are estimated by the data in 0.75-54.4 mbsf of the core.) and statistical error.

We found that the most of data points in 886C are located well above the curves. The iridium abundance of a mixture of Earth's surface material are calculated through three linear combinations of materials of Earth,

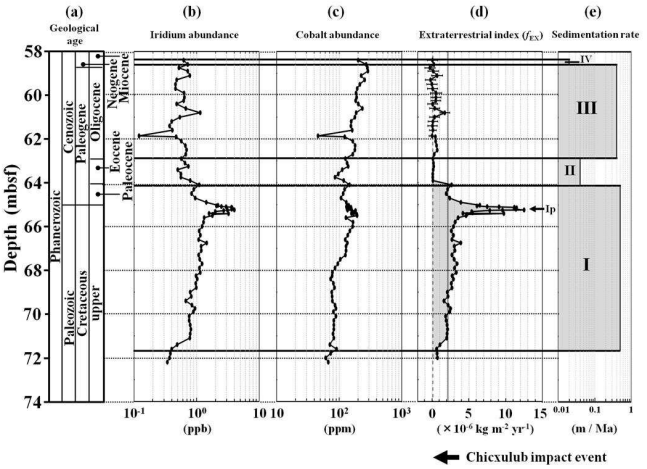

cobalt abundance (c) [4], extraterrestrial index (d), and sedimentation rate (e)[23], as well as the pelagic deep sea sediments sampled at 886C.

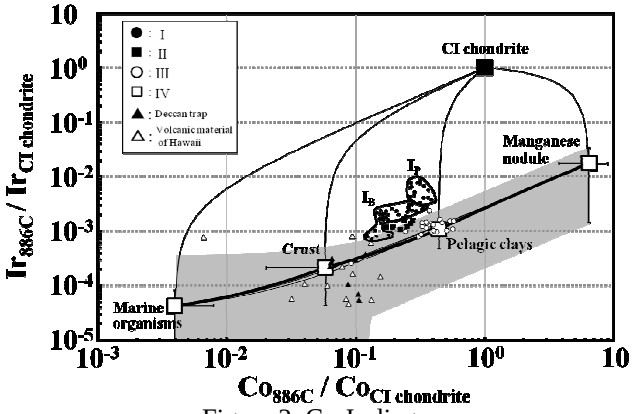

Figure 2. Co-Ir diagram.

including marine organisms (MO), marine crust (MC), pelagic clays (PC), and manganese nodule (MN), with the contribution of exosolar material (Y_{EX}) as:

$$\begin{aligned} Y_{\mathrm{EX}} &= Y-\{(3.0\times10^{-6})\,X+(1.4\times10^{-5})\} \text{ for MO to MC,} \\ &= Y-\{(2.1\times10^{-6})\,X+(4.0\times10^{-5})\} \text{ for MC to PC,} \quad (1) \\ &= Y-\{(2.6\times10^{-6})\,X-(7.3\times10^{-5})\} \text{ for PC to MN,} \end{aligned}$$

where Y and X are iridium and cobalt abundances in ppm. Assuming that the excess iridium abundance in the sediment originates from exsolar materials, the extraterrestrial index f_{EX} can be defined as:

$$f_{\mathrm{EX}} = \nu\, q\left(\frac{Y_{\mathrm{EX}}}{Y_{\mathrm{CI}}}\right) \qquad (2)$$

where v, q, and Y_{CI} are sedimentation speed, a density of the core sample, and the iridium abundance of CI chondrite, respectively. The index f_{EX} gives the flux of extraterrestrial matter at the time of the sedimentation (Fig. 1d). It is worth noting that this iridium-enriched zone continues over 5 m. Neither diffusion nor bioturbation can explain this broad anomaly because of the following reasons: (1) the redistribution of platinum-group-element such as Pt, Re, and Ir is generally less than 10 cm [15], (2) the mean depth of marine bioturbation is as small as ~10 cm [16], which is much less than the width of the broad component (~5 m), and (3) the evidence of bioturbation is minor in the core.

Dark cloud encounter: Fig. 3a shows the estimated flux of exosolar material of 10-80 Ma through equation (1) and (2). We assumed a density of the core sample to be 3 g cm^{-3}. The enhanced flux of exosolar material began ~73 Ma, and has continued to fall through ~8 Myr. The peak at 66 Ma is likely to be originated from an asteroid impact which formed the Chicxulub impact crater [4]. On the other hand, the broad component can be explained not solely by the Chicxulub impact, but by an encounter with a giant molecular cloud. The encounter leads to a "Nebula Winter" [2, 3], in which an environmental catastrophe of the Earth is driven by an enhanced flux of cosmic dust particles and cosmic rays, which cause global cooling and destruction of the ozone layer.

The scale on the right hand side of Fig. 3a denotes the density of nebula N, corresponding to dust flux in the case of relative velocity of the solar system and cloud V is 10 km s^{-1} and 20 km^{-1} by following equation [2]:

$$N = 1000\ \text{protons/cc}\left(\frac{f_{EX}}{1.0\times10^{-8}\ \text{kg m}^{-2}\ \text{yr}^{-1}}\right)\left[1.0\left(\frac{V}{20\ \text{km s}^{-1}}\right)+4.6\left(\frac{V}{20\ \text{km s}^{-1}}\right)^{-1}\right]^{-2} \quad (3)$$

The dark cloud density of 2000-6000 protons/cc corresponds to the climate forcing of snowball earth (-9.3 W m^{-2} [17]), for the case that typical size and density of cosmic dust particles are 0.2 μm and 3 g cm^{-3} . We consider that the broad component can be caused by an encounter of the solar system with a dark cloud with a size of ～80 pc and the central density of over 2000 protons/cc in the galactic disk and estimated that the flux of exosolar material began ～73 Ma and has run through ～8 Myr. This results consistent with the variations of stable isotope ratios in oxygen [18-21] and strontium [5, 18, 22]. The resulting growth of the continental ice sheet also resulted in a regression of the sea level. The global cooling, which appears to be associ ated with a decrease in the diversity of fossils, eventu ally led to the mass extinction at the K-Pg boundary (Fig. 3b).

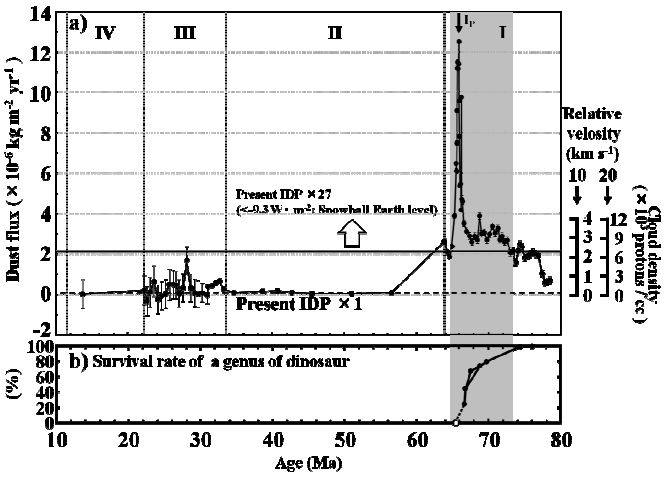

Figure 3. Dust flux and dark cloud density (a). The survival rate of a genus of dinosur [24] (b).

References: [1] Maruyama, S. and Santosh, M. (2008) *GR 14*, 22-32. [2] Kataoka, R. (2013) *New Astron. 21*, 50-62. [3] Kataoka, R. (2014) *GR 25*, 1153-1163. [4] Kyte, F. T. et al. (1995) *Proc. ODP, Sci. Results 145*, 427-434. [5] Ingram, B. L. (1995) *Proc. ODP, Sci. Results 145*, 399-412. [6] Martic, M. et al., (1980) *JRNC 59*, 445-451. [7] Wells et al., (1988) *GCA 52*, 1737-1739. [8] Taylor, S. R. and McLennan, S. M. (1985) The Continental Crust: Its Composition and Evolution (312pp.) [9] Goldberg, E. D. et al. (1986) *Appl. Geochem. 1*, 227-232. [10] Terashima, S. et al. (2002) *Bull. Geol. Surv. Japan 53*, 725-747. [11] Glasby, G. P. et al. (1978) *Geochem. J. 12*, 229-243.[12] Harriss R. C. et al. (1986) *GCA 32*, 1049-1056. [13] Usui, A and Moritani, T (1992) *CPCEMR 14*, 205-223. [14] Lodders, K. (2003) *ApJ 591*, 1220-1247. [15] Colodner, D. C. et al. (1992) *Nature 358*, 402-404. [16] Boudreau, B. P. *L&O 43*, 524-526. [17] Pavlov, A. A. et al. (2005) *GRL 32*, L03705. [18] Barrera, E. and Huber, B. T. (1990) *Proc. ODP, Sci. Results 113*, 813-827. [19] Li, L. and Keller, L. (1998) *Mar. Micropaleontol.* 33, 55-86. [20] Li, L. and Keller, L. (1999) *Mar. Geol.* 161, 171-190. [21] Barrera, E.and Savin, S. M. (1999) *GSA Special Paper 332*, 245-282. [22] Sugarman, P. J. et al. (1995) *GSAB 107*, 19-37. [23] Snoeckx, H. et al. (1995) *Proc. ODP, Sci. Results 145*, 219-230. [24] Sloan, R. E. et al. (1986) *Science 232*, 629-633.

Acknowledgements: This work was supported by JSPS KAKENHI Grant Numbers 26106002, 26106006.